Rings and Strain in Pure Silica Zeolites

German Sastre* and Avelino Corma

Instituto de Tecnologia Quimica UPV-CSIC, Universidad Politecnica de Valencia, Avda. Los Naranjos s/n, 46022 Valencia, Spain

Received: January 24, 2006; In Final Form: July 21, 2006

The stability of rings in pure silica zeolite frameworks is investigated through a new method. The energetic terms influencing the stability of rings are evaluated through the short-range plus electrostatics corresponding to SiO bonds and OSiO and SiOSi angles. Several atomistic force fields have been evaluated, and a reparametrization of the Vessal−Leslie−Catlow force field has been chosen because of its physical meaning and good structural accuracy. The ring energetics are analyzed and discussed in terms of local strain in the framework and in terms of geometric variables. This methodology allows to differentiate between the strain of rings of a given size in different zeolite structures. In particular, it is found that double four rings (D4Rs) are not necessarily, as previously stated, a strained secondary building unit. The analyses of D4Rs in the topologies AST, BEC, and LTA allow the calculation of its stability in the different structures showing high energy in BEC and LTA and low energy in AST. Implications of these results on nucleation of zeolites are drawn regarding the facility with which D4Rs are inserted in different frameworks.

1. Introduction

Zeolites are microporous inorganic molecular sieves formed by tetrahedra of silicon, which can also contain other T^{IV} and T^{III} elements (T = tetrahedral) in the framework. These materials have generated much experimental and theoretical work owing to their extraordinary commercial impact in the fields of adsorption and catalysis,[1] as well as in other electronic and medical applications.[2] New zeolites with a large variety of topologies and pore dimensions are synthesized at an accelerated pace in recent years,[3] and concerns have been raised about the stability of large pore crystalline structures based on framework density and rings.[4]

Rings in zeolites are composed of circuits of alternating silicon (or another tetrahedral element) and oxygen atoms. A more strict and topological definition of ring[5] introduces the concept that valid rings are those with no shortcuts (shortcuts are rings inside rings), which means that a valid ring cannot comprise a smaller ring. Rings exist in silica structures and in solution because they contribute electrostatically to the stability of the final material and because of the energy gain due to the extracondensation reactions that take place between ends of silica chains with respect to their uncondensed forms.[6] Apart from these two sources of stability, rings also lead to constraints on the geometry, and this generates an energetic payload. For example, if we consider the OSiO angle fixed at the equilibrium value 109.47°,[7] a planar four-membered ring (4MR) requires SiOSi angles of 160.5°, whereas a planar five-membered ring (5MR) implies 178.5°. Although rings are normally not flat but puckered, geometrical constraints still exist and they introduce strain into the system. Ring constraints are, nevertheless, compensated by the energy gained during the silica polymerization, and they occur in vitreous as well as in ordered silica materials. The number and size of the rings formed depend on a variety of factors defined by the synthesis conditions, and this will influence the final stability of the solid formed. The most stable SiO_2 polymorph is α-quartz which consists exclusively of 6- and 8MRs as indicated by the vertex symbol[5] of its unique Si site (6_16_1 6_26_2 8_78_7). Given any Si atom (vertex) in a zeolite, its four attached oxygens define six possible paths each corresponding to a ring: O_1-Si-O_2, O_1-Si-O_3, O_1-Si-O_4, O_2-Si-O_3, O_2-Si-O_4, and O_3-Si-O_4. The size and multiplicity of the corresponding six rings make the vertex symbol. A simple way to calculate the number of rings of each size per SiO_2 unit is to sum the multiplicities of the vertex symbols divided by the corresponding ring size as follows:

$$\text{number of 6MR/SiO}_2 = {}^1/_6 + {}^1/_6 + {}^2/_6 + {}^2/_6 = 1 \quad (1)$$

$$\text{number of 8MR/SiO}_2 = {}^7/_8 + {}^7/_8 = 1.75 \quad (2)$$

For structures with more than one vertex type, summing up all the different sites with their multiplicities gives the total number of rings of each size per unit cell.

The final number of rings of each size in a zeolite is a compromise between ring stability and topological requirements to form a given four-connected 3-D network and, within this global basis, 8- and 6MRs are among the most common and stable. Cristobalite, a high energy polymorph of quartz (more stable than any zeolite), has a vertex index of 6_26_2 6_26_2 6_26_2, which also points to the stability and topological convenience of 6MRs. Odd-membered rings seem less frequent than even-membered rings, possibly because of topological constraints dictated by the connectivity and dimensionality of tectosilicates. Among the odd-membered rings, the 5MR is the most frequent and stable. While rings of medium size are among the most stable, the presence of small and large MRs is associated to either energetic or topologic penalties. For example, 4MRs may introduce a certain energetic instability owing to the constraint in their SiOSi angles, whereas large rings such as 10- and 12MRs introduce microporosity, and voids cannot be made without increasing the energy of the final solid with respect to

* To whom correspondence should be addressed. E-mail: gsastre@itq.upv.es.

10.1021/jp060505x CCC: $33.50
Published on Web 08/23/2006

the high-density phase.[8] In this sense zeolites are always higher in energy than quartz and other high-density phases of SiO_2 (cristoballite, trydimite, coesite).[9] Larger stability for 6- and 8MRs, should not necessarily be a general rule, and therefore stable geometries and conformations can be found within any ring size. For example, 6MRs are in general stable rings, but structures with many 6 MRs cannot be regarded as stable without first calculating the energies of the rings, which is one of the topics addressed in this study. Therefore the stability of a particular zeolite framework cannot be calculated or guessed from the vertex symbols or T-site loop configurations.[10] At least an attempt has been made to relate framework stability with Si loop configuration,[9] but the correlations found did not improve other correlations of energy based on, for example, framework density.[11] Indeed, the experimental correlation found[11] by drop solution calorimetry in tectosilicates (including zeolites) between framework density and energetic stability has been a milestone and a classic reference point to link structure and stability. This relation was first found in a computational study by Akporiaye and Price[12] and later, in a more systematic study, by Henson et al.[13]

The framework density of tectosilicates has also been related to average ring sizes that lie in the hyperbolic surface of the framework,[14] and this allowed researchers to establish that the framework density increases monotonically with the average ring size and that this correlation is worse if only the smallest rings are considered. A further development in this respect consists on decomposing the zeolite framework in face-sharing polyhedra (polyhedral tiles), from which average face-size and variance of the face-size distribution can be calculated. It has been demonstrated that a correlation exists between viable zeolite structures and variance of the face-size distribution for a fixed average face-size.[15] This represents a major advance that links the energetic stability of framework structures with topological descriptors without an explicit reference to geometric details. Nevertheless, a considerable number of tile isomers (which correspond to nonviable structures) exist which do not follow the observed correlation. This indicates that still the present topological approach, despite its major interest, needs additional information that takes into account the tile arrangements, which relates to the way tiles are packed together.

Apart from the importance of the global topological descriptors described above, a parallel approach comes back to the more traditional use of geometry to relate framework structure and energetics, which leads us to the study of bonds in silicates.[16] A general observation in zeolites is that almost rigid tetrahedra, $SiO_{4/2}$, can move and reorient without excessive strain, and the existence of RUMs (rigid unit modes), characterized by specific very low or nearly zero vibration frequencies, show the known feature that OSiO angles are rather rigid whereas SiOSi are flexible.[17] In pure silica structures, most OSiO angles lie within 105−115° whereas SiOSi vary within 135−180°. Local bonding forces in siloxane clusters and solid silicates are believed to be similar, and hence the flexibility of those angles in zeolites can be related to that of their cluster counterparts.[18] From quantum chemical calculations, an equilibrium curve of energy versus SiOSi angle has been presented, whose minimum is at a SiOSi angle which depends on the SiO distance. Decreasing SiO distances shift the minimum energy SiOSi angle toward increasing values, and a correlation between SiO distances and minimum energy SiOSi angles has been proposed and justified in terms of hybridization concepts based on the s-character of the SiO bond.[19] Small differences in zeolite stability have been ascribed to the distribution of SiOSi angles.[11] Nevertheless, average SiOSi angles do not correlate with energies because the curve of energy versus SiOSi angle cannot be taken as a straight line within the range 130−180°, which is the range most commonly found in zeolite structures. On the other hand, a linear approximation between energy versus angle can be done in the narrower range of SiOSi angles below 140° and then, when the number of SiOSi angles below that value is plotted against experimental energies (enthalpies), a straight line is obtained.[11] Although this is only a crude approximation, the simplicity of the argument and the quality of the correlation justifies the approach and validates the concept behind.

Along a similar line, the Atlas of Zeolite Structure Types[20] includes, based on work by Brunner,[10] a plot of the framework density versus percentage of (3 + 4)MR present in the structure, structures of increasing density allowing an increasing fraction of (3 + 4)MR. The scattered points do not follow a straight line but rather they define a lower limit for the framework density below which structures cannot be synthesized at a given value of (3 + 4)MR abundance. If we consider that framework density varies more or less linearly with enthalpy of formation, and that the percentage of (3 + 4)MR is closely related to angles smaller or equal than 140°, then the connection between the two above approaches becomes clear. Nevertheless, the quality of the correlations can be improved if a more rigorous approach is developed, and this is the purpose of this work.

In this sense, we are interested in obtaining a better understanding of what makes a structure stable or unstable, by developing a more exact selection of variables. We develop a software implemented approach to locate individual rings in any zeolite structure and to calculate their strains from mathematical functions of energy depending on SiO distances, and OSiO and SiOSi angles. Further, we apply this approach to certain special cases that illustrate particular features of zeolite structures that explain the sources of stability and instability in some structures.

2. Methodology and Models

2.1. Ring and Si-Site Strains. Vertex symbols[5] provide a complete way of characterizing rings present in a zeolite structure, and they can be calculated by any version of zeoTsites.[21] The new features in the code include that once a valid ring is found, the atoms comprising it are stored as well as the corresponding relevant structural parameters, distances, and angles.

Once rings are found by the code, their associated energy is calculated through a mathematical function whose qualitative parameter dependence is shown below:

$$E_{\text{ring}} = \sum_{\text{O}_i\text{Si}_j\text{O}_k} E(r_{\text{SiO}}, \theta_{\text{OSiO}}) + \sum_{\text{Si}_i\text{O}_j\text{Si}_k} E(r_{\text{SiO}}, \theta_{\text{SiOSi}}) \qquad (3)$$

where the sum extends over the "*n*" OSiO and "*n*" SiOSi angles present inside a ring of size "*n*" (*n*MR, i.e., formed by "*n*" SiO units). Care is taken that, because rings are associated to each Si site, they are counted only once. Here, for the calculation of energy, we choose a force field approach because it allows easy decomposition of the energy associated to rings through the above components. Further, this methodology has been widely used with success for similar studies over the past decades.[22]

Two types of information are then processed. On one hand, it classifies all the OSiO angles of a given structure according to the ring size to which they belong, and the same is done for SiOSi angles. On the other hand, it calculates the strain (energy) associated to each individual ring in the framework which contains two separate terms, the OSiO and the SiOSi parts. Also,

TABLE 1: Comparison of the Experimental and Calculated Structural Properties of α-Quartz[a]

α-quartz[b]	exptl	calcd	α-quartz[b]	exptl	calcd	α-quartz[b]	exptl	cald
a	4.9021	4.9024	C_{33}	10.5750	11.3142	Si−O	1.613	1.612
c	5.3997	5.4080	C_{44}	5.8200	4.8590	Si−Si	3.053	3.057
Si(x)	0.4680	0.4656	C_{66}	3.9900	3.8318	Si−O−Si	142.4	140.1
O(x)	0.4124	0.4100	ϵ_{11} (static)	4.5200	3.3150	O−Si−O	110.7	111.0
O(y)	0.2712	0.2766	ϵ_{33} (static)	4.6400	3.5305		108.9	108.4
O(z)	0.2170	0.2226	ϵ_{11} (high frequency)	2.4000	1.9120		108.6	108.4
C_{11}	8.6800	9.1826	ϵ_{33} (high frequency)	2.4000	1.9271		108.6	108.4
C_{12}	0.7040	1.5190	frequency	1162.0000	1131.4483		109.4	109.7
C_{13}	1.1910	1.6667	cell volume	112.3737	112.5607		110.7	111.0
C_{14}	−1.8040	−1.7234						

[a] Cell parameters, atomic distances, and coordinates in Å; bulk modulus in GPa; cell volume in Å^3; bond angles in degrees; elastic constants in GPa; and frequencies in cm^{-1}. Note that the frequency quoted here is the maximum value at the point. The force field in Table 2 has been used to obtain the calculated values. [a] Space group: $P3_121$ (No. 152).

the strain associated to each individual Si site in the structure is calculated as follows:

$$E_{\text{Si-site}} = \sum_{\text{O}_i\text{SiO}_k} E(r_{\text{SiO}}, \theta_{\text{OSiO}}) \tag{4}$$

where the sum extends to the six OSiO angles associated to each Si site and there it is implicit that the source of strain comes from deformation of such angles of the tetrahedra.

2.2. Force Field Considerations. The choice of a good force field is critical and its quality can be tested by testing how it reproduces certain experimental data, and as we are interested in structural features, the cell parameters will be used.

2.2.1. Atomistic Force Field. A number of previously fitted force fields have been analyzed in order to check which one is the best suited for the purpose of this work, or which one is the best to be used after a reparametrization aimed for a better performance. The force field by Sanders et al.[23] cannot be used because it does not contain an explicit SiOSi energy term that we need in order to evaluate the energy of rings, and the same happens with the force field by Metiu et al.[24] The recently parametrized force field for all silica zeolites by Goddard et al.[25] only contains two body terms and does not allow an evaluation of eq. 3. A force field by Huang et al.[26] contains a three-body term which is symmetric with respect to the equilibrium angle and this does not seem an appropriate behavior for the SiOSi angle. The force field by Rösch et al.[27] contains harmonic terms for OSiO and SiOSi but the respective force constants are 0.90 and 5.62 eV/rd^2 which is against the experimental observation that SiOSi angles are more flexible than OSiO angles. The force field by Barkema et al.[28] does contain the right balance between the force constants for SiOSi and OSiO angles but provides an equilibrium angle for SiOSi equal to 180° which is contrary to what is observed in tectosilicates. Finally, two possible options are the force fields by Vashishta et al.[29] and Vessal et al.[30] We have chosen the latter because of the more simple functional expression. Also, by being a force field for amorphous silica, which are characterized by SiOSi angle distributions measured by ^{29}Si NMR,[31] this force field contains a good balance between OSiO and SiOSi energetics. On the other hand, force constants of siloxanes and silica oligomers are not very different from their equivalent in condensed phases[19] and therefore this force field can also be used for zeolites. Nevertheless, we have decided to reparametrize this force field by changing it from a rigid-ion to a shell-model force field, because in modeling oxide materials, the shell model for the oxygen atoms has proven essential in order to fit dielectric constants, phonons, and other characteristic properties.[32] This is because the polarization of oxygen may also act to mimic covalency effects that would lead to lower ionic charges than the formal ones, which are chosen in the present study and many previous ones.

The reparametrization has been performed by keeping the three-body term parameters and taking the core−shell charge split as well as the core−shell harmonic force constant from a similar force field.[23] The rest of the parameters have been allowed to vary and the structure of α-quartz as well as some of its physicochemical properties (see Table 1) have been chosen for the fit. To obtain a good quality fit, it is vital to incorporate data regarding the curvature of the energy surface about the minima. Hence, apart from the structure, other observables included are the bulk moduli as well as the elastic constants and the highest phonon frequency.

The following terms and functional forms have been considered:

$$E_{\text{zeo}} = E_{\text{Coulombic}} + E_{\text{Buckingham}} + E_{\text{three-body}} + E_{\text{core-shell}} \tag{5}$$

$$E_{ij}^{\text{Coulombic}} = \frac{q_i q_j}{4\pi\epsilon_0 r_{ij}} \tag{6}$$

$$E_{ij}^{\text{Buckingham}} = A_{ij}\exp\left(-\frac{r_{ij}}{\rho_{ij}}\right) - \frac{C_{ij}}{r_{ij}^6} \tag{7}$$

$$E_{ijk}^{\text{three-body(TOT)}} = \frac{1}{8}\frac{k_{ijk}^{\theta}}{(\theta_0 - \pi)^2}((\theta_0 - \pi)^2 - (\theta_{ijk} - \pi)^2)^2 \exp\left(-\frac{r_{ij}}{\rho}\right)\exp\left(-\frac{r_{jk}}{\rho}\right) \tag{8}$$

$$E_{ijk}^{\text{three-body(OTO)}} = \frac{1}{2}k_{ijk}^{\theta}(\theta_{ijk} - \theta_0)^2 \tag{9}$$

$$E_{ij}^{\text{core-shell}} = \frac{1}{2}k_{ij}^{\text{cs}} r_{ij}^{\ 2} \tag{10}$$

We note that the three-body term has the feature of reproducing different bending curves depending on the values of the SiO distances (included in the exponential term), and this is in agreement with the results by Newton and Gibbs.[19] We have used the relaxed fitting scheme[32] for the final refinement of the potential parameters, as implemented within the GULP[33] program. Here the structure of every phase is minimized at each point of the least-squares procedure and the displacements from the experimentally observed structure form the basis of the residuals, instead of just using the forces acting on the structure at the experimental geometry. Similarly, the curvature related properties are evaluated at the optimized structure since this is more reliable and formally correct.

TABLE 2: New Interatomic Potential Parameters for Pure Silica Zeolites[a]

Atomic Charges (Equation 6)

atom	core	shell	ref
Si	4.0	no shell	23
O	0.86902	−2.86902	23

Buckingham (Equation 7)

i	*j*	A_{ij} (eVÅ^{12})	θ_{ij} (Å)	C_{ij} (eVÅ^6)	ref
O shell	O shell	2046.0422	0.134015	14.027	this work
Si core	O shell	1824.2944	0.289798	0.000	this work

Three Body (Equation 8 for SiOSi and Equation 9 for OSiO)

i	*j*	*k*	k^{θ}_{ijk} (eV rad^{-2})	θ_0 (deg)	ρ (Å^{-1})	ref
Si core	O shell	Si core	729.1	144.00	0.3277	30
O shell	Si core	O shell	2.0972	109.47		23

Spring (Equation 10)

i	*j*	k^{cs}_{ij} (eVÅ^{-2})	ref
O core	O shell	74.92	23

[a] This force field is a modification of the force field by Vessal et al.[30] from which the atomic charges and the three body terms have been taken. Then, the core−shell charge split and force constant for the oxygen atoms has been taken from the force field by Sanders et al.[23] The Buckingham terms have been adjusted in the fit to reproduce the properties of α-quartz (see Table 1).

The quality of a fit can be measured by the sum of the squares of the differences between the experimental and calculated values for the observables, multiplied by appropriate weighting factors. Here the weights used are 1000.0 for all unit cell parameters, 10000.0 for all fractional coordinates, and 1.0 for all properties. This reflects the fact that it is pointless to reproduce the curvature related properties unless the structure is first reproduced. A final sum of squares of 7.5 is obtained within the above model which corresponds to a reasonable quality for the fit. The final parameters of this new force field are shown in Table 2.

Once the parametrization is completed, energy minimizations were performed in order to examine the ability of the force field to reproduce the structures of four zeolite structures which were not included in the original fit, thereby providing a test of the transferability (see Table 3), and the results show a reasonable behavior within 4% of error in the cell parameters of the structures tested.

2.2.2. Molecular Force Field. While we have used the previous atomistic force field for our entire analysis, we have additionally chosen the possibility to parametrize a second force field, of molecular nature, in this study. A molecular force field considers bonds within selected pairs or groups of atoms attending to the specific nature of the interactions in the system. The reason for this choice is the advantage of comparing results with two force fields and also to see what features and reproducibility of the results can be modeled when some of the energetic terms of the different force fields have a completely different nature. The parametrization procedure followed was entirely similar to that described above, and the particularities of the new force field will be explained later.

2.3. Models. We will take pure silica zeolites whose structures have been determined by accurate XRD or synchrotron data and for our ring analysis we will consider only the experimental data, thus we will not minimize the structures with our force field, but rather we will only use the force field to calculate the energetic terms related to our analyses. The zeoTsites software[34] locates rings and finds the ring size to which all the three-body angles (OSiO and SiOSi) belong to, and also it calculates the strain associated to both the rings (see eq 3) and the Si sites (see eq 4), provided the necessary energy expressions are included in the corresponding subroutine. In our particular case, the eqs 8 and 9, with the corresponding parameters for the OSiO and SiOSi cases (see Table 2), are substituted in eqs 3 and 4 and this allows the calculation of the strain energies.

TABLE 3: Cell Parameters of Pure Silica ITQ-4[48] (IFR), ITQ-29 (LTA),[43c] ITQ-1[49] (MWW), and SSZ-33[50] (CON) Zeolites (Distances in Å, Angles in deg) Obtained Experimentally and Comparison of Results Obtained with the Sanders et al.[23] Force Field (ff) and with the Force Field Parameterized in This Study (Table 2)

	a	*b*	*c*	α	*β*	*γ*
ITQ-4 (exptl, ref 48)	18.6524	13.4960	7.6311	90.0	101.98	90.0
ITQ-4 (Sanders ff)	18.5766	13.4235	7.6321	90.0	101.68	90.0
ITQ-4 (new ff)	18.8387	13.5425	7.7266	90.0	101.68	90.0
LTA (exptl, ref 43)	11.8671	11.8671	11.8671	90.0	90.00	90.0
LTA (Sanders ff)	11.8277	11.8277	11.8277	90.0	90.00	90.0
LTA (new ff)	11.9542	11.9542	11.9542	90.0	90.00	90.0
ITQ-1 (exptl, ref 49)	14.2081	14.2081	24.9450	90.0	90.00	120.0
ITQ-1 (Sanders ff)	14.2383	14.2383	24.9062	90.0	90.00	120.0
ITQ-1 (new ff)	14.3929	14.3929	25.1754	90.0	90.00	120.0
SSZ-33[a] (exptl, ref 50)	22.6242	13.3503	12.3642	90.0	68.91	90.0
SSZ-33 (Sanders ff)	22.6547	13.4068	12.3944	90.0	68.64	90.0
SSZ-33 (new ff)	22.9136	13.5539	12.5293	90.0	68.77	90.0

[a] This corresponds to the CON topology of the SSZ-26/SSZ-33/CIT-1 family of zeolites, which in the original publication by Lobo et al. (ref 50) is referred to as polymorph B.

3. Results and Discussion

3.1. Are the Si Sites Associated to 3MR the Most Strained in the ZSM-18 Structure? ZSM-18[35] (with MEI topology[36]) was the first and one of the few current zeolite materials synthesized containing 3MRs. Prior to the synthesis of ZSM-18, these rings had been found in vitreous silica and were known to be very strained, to the point that serious concerns about its accommodability in a tectosilicate were raised.[37] Something that releases partially the strain of 3MRs is the possibility of introducing certain heteroatoms (tetrahedral atoms other than Si), and, in fact, a preferential location of Al in the 3MR of ZSM-18 has been found experimentally.[35] The structure of ZSM-18 contains a tridirectional microporous space defined by two crossing channel systems of a 7MR (3.2 × 3.5 Å, intercrossing two-dimensional, perpendicular to [001]) and a 12MR (6.9 × 6.9 Å, parallel to [001]) channels. The $P6_3/m$ (No. 176) unit cell, framework, is $[Al_xSi_{34-x}O_{68}]$, with x in the range between 2.1 and 5.7. There are four inequivalent T sites whose vertex symbols (see caption in Table 4) indicate that the 3MRs are made of 3 Si4 sites (Figure 1).

A previous computational study[38] shows that, when the template is used in the calculation, the Si4 is the position where Al tends to locate, owing mainly to electrostatic interactions with the triply charged template used in the synthesis.[39] Nevertheless, when the template is not taken into account and defect calculations (which refer to the Si → Al substitution) are performed, it is found that the Si4 site is the less favorable position,[38] and the same result was also found by Gale and Cheetham.[40] Therefore, it seems that from the framework viewpoint (not taking into account framework-template interactions), Al atoms in the 3MR are the most strained. However, a different picture may emerge without the electrostatic part. The Si → Al substitution is not electrically neutral, and electrostatic factors may be playing an important role in the energetics. We are interested here in calculating the strain associated to each

TABLE 4: Ring Analysis of the Pure Silica ZSM-18[a] (MEI) Structure (Angles in deg, Distances in Å, Energies in kcal/mol)

T−O−T labels			T−O−T	rings (multip)[b]	TOT-strain/ O-atom	number
Si1	O5	Si1	180.0	7 (3)	0.62	2
Si12	O6	Si2	147.4	4 (2) 7 (1)	0.01	12
Si2	O7	Si3	150.9	4 (2) 5 (1)	0.06	12
Si2	O8	Si3	142.6	4 (1) 5 (1) 12 (1)	0.00	12
Si2	O11	Si3	147.7	4 (1) 7 (1) 12 (1)	0.02	12
Si3	O9	Si4	149.6	5 (2) 7 (1)	0.04	12
Si4	O10	Si4	134.7	3 (1) 5 (2)	0.13	6

O−T−O labels			O−T−O	rings (multip)[b]	OTO-strain/ T-atom	number
O5	Si	O6	112.0	7 (1)	0.10	12
O6	Si1	O6	106.9	4 (1)	0.10	12
O6	Si2	O7	111.0	4 (1)	0.03	12
O6	Si2	O8	109.8	4 (1)	0.00	12
O6	Si2	O11	110.3	7 (1)	0.01	12
O7	Si2	O8	107.8	5 (1)	0.04	12
O7	Si2	O11	108.4	4 (1)	0.02	12
O8	Si2	O11	109.5	12 (1)	0.00	12
O7	Si3	O8	107.9	4 (1)	0.04	12
O7	Si3	O9	109.5	5 (1)	0.00	12
O7	Si3	O11	109.8	4 (1)	0.00	12
O8	Si3	O9	110.0	5 (1)	0.00	12
O8	Si3	O11	110.4	12 (1)	0.01	12
O9	Si3	O11	109.1	7 (1)	0.00	12
O9	Si4	O9	111.9	7 (1)	0.10	6
O9	Si4	O10	109.8	5 (1)	0.00	24
O10	Si4	O10	105.3	3 (1)	0.26	6

T label	O−T−O	number
Si1	109.416	24
Si2	109.464	72
Si3	109.472	72
Si4	109.439	36

T label	OTO-strain/T-atom	number
Si1	0.60	4
Si2	0.11	12
Si3	0.06	12
Si4	0.36	6

Three-Body Strain Energy (kcal/mol) in the Different Ring Types

	3MR	4 MR type 1	4MR type 2	5MR	7MR	12MR
OTO-strain in ring/T-atom	0.257	0.045	0.011	0.012	0.046	0.007
TOT-strain in ring/O-atom	0.157	0.024	0.041	0.061	0.110	0.011
3-body-strain in ring/T-atom	0.415	0.069	0.051	0.073	0.156	0.019

[a] ZSM-18, IZA code: MEI. Space group: *P*63/*m* (No. 176). Cell parameters as in ref 35: $a = 13.175$ Å, $c = 15.848$ Å. Unit cell: $Si_{34}O_{68}$. Ring atom types as follow: Si4 O10 Si4 O10 Si4 O10 (3MR); Si3 O7 Si2 O6 Si1 O6 Si2 O8 (4MR, type 1); Si2 O7 Si3 O11 Si2 O7 Si3 O11 (4MR, type 2); Si4 O10 Si4 O9 Si3 O8 Si2 O7 Si3 O9 (5MR); Si3 O9 Si4 O9 Si3 O11 Si2 O6 Si1 O5 Si1 O6 Si2 O11 (7MR); Si2 O8 Si3 O11 Si2 O8 Si3 O11 Si2 O8 Si3 O11 Si2 O8 Si3 O11 Si2 O8 Si3 O11 Si2 O8 Si3 O11 (12MR). Vertex symbols as follow:

label	vertex symbol	Number
Si1	$4_1\ 7_1$ $4_1\ 7_1$ $4_1\ 7_1$	4
Si2	$4_1\ 4_1$ $4_1\ 12_1$ $5_1\ 7_1$	12
Si3	$4_1\ 5_1$ $4_1\ 7_1$ $5_1\ 12_1$	12
Si4	$3_1\ 7_1$ $5_1\ 5_1$ $5_1\ 5_1$	6

[b] This refers to rings comprising the corresponding OSiO or SiOSi angle. In the OSiO case, only one ring size corresponds to one angle, but in the case of a SiOSi angle, several ring sizes can share the same SiOSi. The corresponding multiplicity (multip) is indicated between parenthesis.

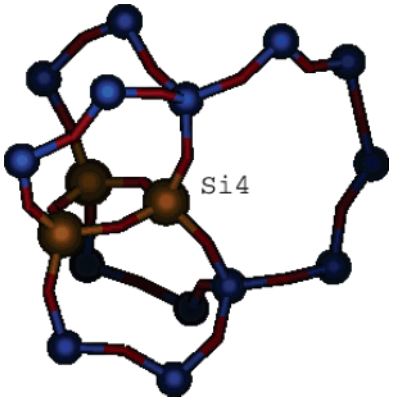

Figure 1. Detail of the ZSM-18 structure showing a 3MR (formed by 3 Si4 atoms) and the rings associated to a Si4 (one 3MR, four 5MR and one 7MR).

Si site and instead a defect calculation, a calculation of the strain associated to each Si site, is necessary. Starting from a pure silica MEI structure and taking into account the eqs 4 and 9, zeoTsites can calculate the strain associated to each Si site. The strain energies are shown in Table 4, as well as the average OSiO angles for each case. It is seen that although Si sites corresponding to 3MR are quite strained (0.36 kcal/mol), the Si1 site is still more strained (0.60 kcal/mol) as it corresponds to the OSiO angles farther from the equilibrium than those corresponding to the other Si sites (Table 4). The fact that the Si sites corresponding to the 3MR are not the most strained may seem like a striking result in the sense that 3MR are always seen as the most strained, but a simple explanation for that follows. The Si sites forming the 3MR contain six OSiO angles, of which only one belongs to the 3MR (see vertex symbols of Si4 in caption of Table 4 and Figure 1). Even considering that this angle corresponds to a strained ring, there are another five components in the total strain associated to a tetrahedral position. Although the most strained position, Si1, does not contain any OSiO corresponding to a 3MR, it contains two terms associated to strained 7MR rings, which in turn become more globally important than the 3MR term in the Si4 site. If we now look, not to the Si strains (eq 4) but to the ring strains (eq 5) in Table 4, it is found that the 3MRs are clearly the most unstable, followed by the 7MRs. It follows from this that a distinction among the reasons why a structure is strained may include at least two different, although related, sources of strain: Si sites and rings.

3.2. Why the Faujasite Structure is So High in Energy. The calorimetric study of pure silica structures by Petrovic et al.[11] shows the relation between framework density and structure stability (measured through enthalpies relative to quartz), and it is seen that structures of low density such as faujasite are high in energy. The large pores present in faujasite should not be seen as a justification for the high energy of the structure. Large pores do not lead to low density if other parts of the structure are particularly dense, and conversely, small pore structures can be of low-density such as the case of chabasite.[11] On the other hand, larger rings do not necessarily mean larger SiOSi angles in the pure silica faujasite structure.[41] This analysis also indicates that OSiO angles are reasonably around the equilibrium value except some angles ca. 111.6°, which correspond to O3SiO4 (Table 5). The interesting thing about this strained OSiO angle is that one of the 4MR present in the faujasite is made exclusively of four angles of this kind (see "type 3" in caption of Table 5) and therefore a certain strain accumulates in this ring. Table 5 shows the five different kinds of rings present in the faujasite structure and their corresponding

TABLE 5: Ring Analysis of Pure Silica Faujasite[a] (FAU[41]) Zeolite (Angles in deg, Distances in Å, Energies in kcal/mol)

T−O−T labels			T−O−T	rings[b]	TOT-strain/ O-atom	number
Si	O1	Si	138.4	4 (2) 12 (1)	0.06	96
Si	O3	Si	145.8	4 (2) 6 (1)	0.01	96
Si	O2	Si	149.4	4 (1) 6 (2)	0.04	96
Si	O4	Si	141.4	4 (1) 6 (1) 12 (1)	0.01	96

O−T−O labels			O−T-O	rings[b]	OTO-strain/T-atom	number
O1	Si	O2	110.6	4 (1)	0.02	192
O1	Si	O3	109.1	4 (1)	0.00	192
O1	Si	O4	108.3	12 (1)	0.02	192
O2	Si	O3	108.7	6 (1)	0.01	192
O2	Si	O4	108.7	6 (1)	0.01	192
O3	Si	O4	111.6	4 (1)	0.07	192

T label	T−O−T	T−O	T−T	number
Si	143.756	1.606	3.050	68

T label	O−T−O	number	T label	OTO-strain/T-atom	number
Si	109.475	1152	Si	0.14	192

Three-Body Strain Energy (kcal/mol) in the Different Ring Types:

	4MR type 1	4MR type 2	4MR type 3	6MR	12MR
OTO-strain in ring/T-atom:	0.012	0.011	0.073	0.010	0.024
TOT-strain in ring/O-atom:	0.041	0.041	0.008	0.023	0.034
3-body-strain in ring/T-atom:	0.053	0.052	.081	0.034	0.059

[a] Faujasite. IZA code: FAU. Space group: *Fd*-3*m* (No. 227). Cell parameter: $a = 24.2576$ Å. Unit cell: $Si_{192}O_{384}$. Vertex symbol: Si: $4_1\ 4_1\ 4_1\ 6_1\ 6_1\ 12_1$. Ring atom types as follow: Si O1 Si O3 Si O1 Si O2 (4MR, type 1); Si O1 Si O2 Si O1 Si O3 (4MR, type 2); Si O3 Si O4 Si O3 Si O4 (4MR, type 3); Si O2 Si O3 Si O2 Si O3 Si O2 Si O3 Si O2 (6MR); Si O1 Si O4 Si O1 Si O4 Si O1 Si O4 Si O1 Si O4 Si O1 Si O4 Si O1 Si O4 (12MR). [b] As in Table 4.

strain, with the components in OSiO and SiOSi. Another source of strain in the faujasite structure can be detected in the SiOSi angles less than 140°, and SiO1Si angles with the value 138.4°, forming part of the 4MR of types 1 and 2 (2 SiOSi angles per ring are of the type SiO1Si, see caption of Table 5) and the 12MR (6 SiOSi angles per ring are of the type SiO1Si, see caption of Table 5). Overall, it is shown that an analysis of both the OSiO and the SiOSi angles is necessary to identify the sources of strain in the faujasite structure rather than using SiOSi angles only to asses the stability of a zeolite structure.

3.3. Is the Presence of Double Four Rings or Its Insertion in the Structure a Destabilizing Factor To Obtain a Zeolite Structure? A number of new zeolite structures containing double four ring (D4R) units have been synthesized by a systematic use of the fluoride route first introduced by Flanigen and Patton,[42] and these include the following recently found new topologies and materials (see ref 20): BEC, ITH, IWW, ITQ-21, ASV, IWR, UTL, ISV, ITW, UOZ, ITQ-32, and also ITQ-29 which corresponds not to a new topology but to the already known LTA topology. Other topologies with D4R were synthesized earlier such as AST, LTA, and ACO.[43] Not all of them have been synthesized in the presence of F^- ions, but it is clear that fluoride anions stabilize the formation of D4R units[44] and their insertion in the zeolite structure. Another source of stabilization is the presence of GeO_2 in the synthesis gel, the reason usually argued being that Ge atoms stabilize the TOT (T = Si, Ge) angles required to insert the D4R units in zeolites. To check this assertion, an analysis of different D4Rs in different zeolites is performed, and the aim is to see whether these units contain SiOSi angles below the equilibrium (ca. 145°), that would be more favorable for TOGe links (T = Si, Ge).[45] The

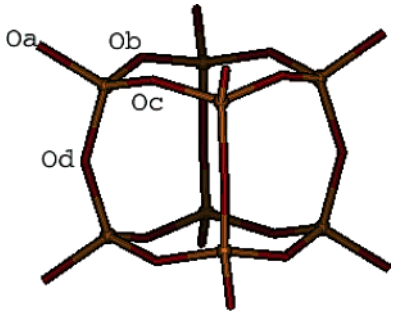

Figure 2. Double four ring (D4R) unit. Six OSiO angles (Oa−Si−Ob, Oa−Si−Oc, Oa−Si−Od, Ob−Si−Oc, Ob−Si−Od and Oc−Si−Od) and four SiO bonds are at each vertex and twelve SiOSi angles form the edges of the D4R.

TABLE 6: Strain Energy (in kcal, with Components in OSiO and SiOSi as Defined in Equations 8 and 9) in the D4R Unit of Pure Silica Octadecasil[51] (AST), β-C[52] (BEC), and ITQ-29[43c] (LTA) Zeolites[a]

	D4R-strain energy terms		
	OSiO	SiOSi	total
AST	0.47	0.15	0.61
BEC	0.00	1.72	1.72
LTA	0.81	0.22	1.03

[a] The terms considered in the D4R are 48 OSiO and 12 SiOSi angles (see Figure 2).

well determined calcined pure silica AST, BEC, and LTA zeolites have been selected for our study of D4Rs. The elements in the strain components of the D4R (Figure 2) are 12 SiOSi angles (forming the edges of the cube) and 48 OSiO angles (6 OSiO angles per each Si), and from them we have calculated the strain energy for each D4R as shown in Table 6. The strain energies allow a comparison of the D4R strain, owing to the OSiO part, with typical OSiO strains in other structures, and the same happens in the SiOSi case. For example, if we compare the OSiO (per T-atom) D4R strain in Table 6 with the OSiO strains (per T-atom) in Tables 4 and 5 we see that OSiO angles in the D4Rs of AST, BEC, and LTA are not particularly high in energy. The same comparison for the SiOSi part shows that the values are below the average strains in zeolites, except in the case of the BEC structure. This means that the D4Rs in the AST and LTA structures do not really pose any particular strain to the formation of the structure. A different picture appears in the case of the BEC structure where it is noted that the D4R is energetically unfavorable (see the value 1.72 kcal in Table 6). To further support these conclusions, some geometry parameters of the three structures are shown in Table 7. In the case of AST it can be seen that all the SiOSi angles taking part in the D4R (Si1O1Si1 and Si1O3Si1) are in the range 146−148°, which is quite close to the equilibrium, and the same is observed with the OSiO angles taking part in the D4R (O1Si1O2, O1Si1O3, O1Si1O1 and O2Si1O3) which are all of them within 108−111°. In the case of LTA it can also be seen (Table 7) that the SiOSi angles involved in the D4R (SiO1Si and SiO3Si) are close to the equilibrium, and the same is observed with the OSiO angles of the D4R (O1SiO2, O1SiO3, O2SiO3 and O3SiO3), within 107−111°, quite close to the equilibrium value. On the other hand, the BEC structure, although it shows OSiO angles very close to the equilibrium, contains SiOSi angles within the D4R (Si1O6Si1, Si1O4Si1 and Si1O3Si1) whose values are far from the equilibrium. Indeed, two of those SiOSi angles show values favorable for TOGe links (T = Si, Ge) as follows: Si1O6Si1 = 136.1° and Si1O4Si1 = 138.9°. This indicates that the D4R is a constraint for the formation of the pure silica BEC

TABLE 7: Ring Analysis of Pure Silica Octadecasil[a] (AST), β-C[b](BEC), and ITQ-29[c] (LTA) Zeolites (Angles in deg, Distances in Å, Energies in kcal/mol)

AST

T−O−T labels			T−O−T	rings[d]	TOT-strain/ O-atom	number	T−O−T labels			T−O−T	rings[d]	TOT-strain/ O-atom	number
Si1	O2	Si2	151.7	6 (3)	0.07	16	Si1	O3	Si1	146.5	4 (2) 6 (1)	0.01	8
Si1	O1	Si1	147.2	4 (2) 6 (1)	0.01	16							

O−T−O labels			O−T−O	rings[d]	OTO-strain/ T-atom	number	O−T−O labels			O−T−O	rings[d]	OTO-strain/ T-atom	number
O1	Si1	O2	108.8	6 (1)	0.01	32	O2	Si1	O3	108.6	6 (1)	0.01	16
O1	Si1	O3	110.0	4 (1)	0.01	32	O2	Si2	O2	109.5	6 (1)	0.00	24
O1	Si1	O1	110.5	4 (1)	0.02	16							

T label	OTO-strain/T-atom	number	T label	OTO-strain/T-atom	number
Si1	0.06	16	Si2	0.03	4

BEC (Newsam et al., ref 52)[e]

T−O−T labels			T−O−T	rings[d]	TOT-strain/ O-atom	number	T−O−T labels			T−O−T	rings[d]	TOT-strain/ O-atom	number
Si1	O6	Si1	136.1	4 (2) 6 (1)	0.12	16	Si2	O2	Si3	148.2	5 (3) 6 (1)	0.02	16
Si1	O4	Si1	138.9	4 (2) 12 (6)	0.04	8	Si2	O1	Si2	136.5	4 (1) 5 (2)	0.08	4
Si1	O3	Si1	163.5	4 (2) 5 (1)	0.27	8	Si2	O7	Si2	175.4	4 (1) 6 (2)	0.36	4
Si1	O5	Si3	149.4	5 (1) 6 (1) 12 (5)	0.03	8							

T label	T−O−T	T−O	T−T	number	T label	T−O−T	T−O	T−T	number
Si1	146.975	1.616	3.085	64	Si2	152.069	1.616	3.112	32
Si3	148.820	1.616	3.113	32					

T label	O−T−O	number	T label	O−T−O	number
Si1	109.471	96	Si2	109.471	48
Si3	109.471	48			

LTA

T−O−T labels			T−O−T	rings[d]	TOT-strain/ O-atom	number	T−O−T labels			T−O−T	rings[d]	TOT-strain/ O-atom	number
Si	O1	Si	147.7	4 (2) 8 (1)	0.02	12	Si	O2	Si	156.9	6 (2) 8 (1)	0.17	12
Si	O3	Si	147.5	4 (2) 6 (1)	0.02	24							

O−T−O labels			O−T−O	rings[d]	OTO-strain/ T-atom	number	O−T−O labels			O−T−O	rings[d]	OTO-strain/ T-atom	number
O3	Si	O1	110.2	4 (1)	0.01	48	O3	Si	O3	109.4	4 (1)	0.00	24
O3	Si	O2	109.9	6 (1)	0.00	48	O1	Si	O2	107.3	8 (1)	0.08	24

T-label	OTO-strain/T-atom	number
Si	0.10	24

[a] Octadecasil. IZA code: AST. Symmetry group *I*4/*m* (No. 87). Cell parameters: $a = 9.255$ Å, $c = 13.501$ Å. Unit cell: $Si_{20}O_{40}$. Vertex symbols as follows:

label	vertex symbol	Number
Si1	$4_1\ 6_1$ $4_1\ 6_1$ $4_1\ 6_1$	16
Si2	$6_1\ 6_1$ $6_1\ 6_1$ $6_1\ 6_1$	4

[b] β-C zeolite. IZA code: BEC. Symmetry group $P4_2/mmc$ (No. 131). Cell parameters: $a = 12.81$ Å, $c = 13.00$ Å. Unit cell: $Si_{32}O_{64}$. Vertex symbols as follows:

label	vertex symbol	Number
Si1	$4_1\ 5_1$ $4_1\ 6_1$ $4_1\ 12_6$	16
Si2	$4_1\ 5_2$ $5_1\ 6_1$ $5_1\ 6_1$	8
Si3	$5_1\ 5_1$ $5_2\ 12_5$ $6_1\ 6_1$	8

[c] Zeolite A. IZA code: LTA. Symmetry group Pm-3m (# 221). Cell parameter: $a = 11.87263$ Å. Unit cell: $Si_{24}O_{48}$. Vertex symbols: Si: $4_1\ 6_1\ 4_1\ 6_1\ 4_1\ 8_1$. [d] As in Table 4. [e] The pure silica BEC structure by Terasaki et al.[53] was also used to calculate the strain energy associated to the D4R and the values found were 1.2, 11.1, and 12.3 kcal for the SiOSi, OSiO, and total components of the energy, respectively.

and also indicates that the D4R of BEC could be more easily formed if GeO_2 is introduced in the synthesis because this will stabilize the low TOGe (T = Si, Ge) angles mentioned above. Previous experimental measurements based on drop solution calorimetry to estimate enthalpies of formation of zeolites indicate that the BEC structure is more difficult to obtain in its pure silica form than other structures with D4Rs such as ITQ-7, β, and ITQ-22.[46] The formation of D4Rs during the nucleation

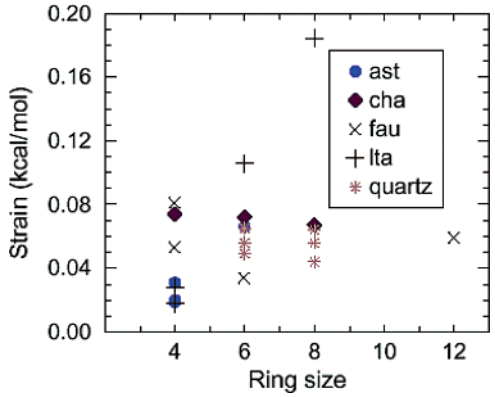

Figure 3. Calculated strain in rings of α-quartz and pure silica AST,[51] CHA,[54] FAU,[41] and LTA[43c] zeolites (see ref 20 for more details of the structure and topology). The quartz structure taken is in Table 1 (experimental set). The force field in Table 2 has been used to obtain the calculated energy values.

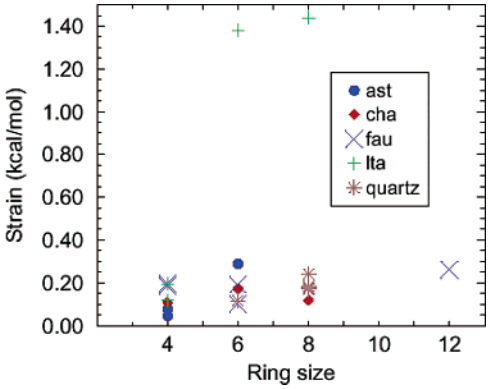

Figure 4. Calculated strain in rings of α-quartz and pure silica AST,[51] CHA,[54] FAU,[41] and LTA[43c] zeolites (see ref 20 for more details of the structure and topology). The quartz structure taken is in Table 1 (experimental set). The SGV force field in Table S2 (see Supporting Information) has been used to obtain the calculated energy values.

of zeolites may explain the difficulties of obtaining pure silica BEC and LTA with respect to AST, the latter having been synthesized much earlier[51] than the recent LTA[43c] and BEC.

The ring analysis tells us that a given secondary building unit in different zeolites is not equally strained or relaxed, and thus the D4R is not in itself a strained building unit as it was suggested elsewhere.[46] The global topology, that is, the way in which the polyhedra are packed together and linked to the zeolite framework makes an important contribution to the final strain or stability of the structure.

3.4. Ring Strain in Some Pure Silica Structures. As a general feature of the methodology, the strain corresponding to all ring types in quartz as well as in pure silica AST, CHA, FAU, and LTA zeolite structures are plotted in Figure 3. It is seen that there is no relation between ring size and energy, and rings of a given size can have significant differences in strain across structures and even within a structure. Further insight into the ring composition shows that there is no relation either between SiOSi average angle values and ring sizes and therefore it is not possible to say, for instance, that SiOSi angles belonging to 4MRs are lower than those belonging to larger MRs. Figure 3 allows the understanding that LTA is difficult to synthesize as a pure silica zeolite[43] because of the relatively high strains in its 6- and 8MRs.

3.5. Are These Results Force Field Dependent? A new force field of different nature to that used all through this study has also been considered for comparison purposes. A simplified general valence (SGV) force field, inspired in a previous study,[47] has been parametrized, and this is based in two main assumptions: (i) that the atoms interact only through bonds, here considering the terms of Si−O bond stretching and Si−O−Si and O−Si−O bond angles, and (ii) that the electrostatic interactions are included within the mentioned terms and therefore Si and O atoms have charges equal to zero. Another point taken into account within our approach, as in the previous force field, is the use of the shell model for the oxygen atoms because of its importance to fit dielectric constants, phonons, and other characteristic properties of the material. Although oxygens have a zero net charge, having plus and minus charged core and shell oxygens provides an improvement over point charges. The structure of α-quartz and some of its physicochemical properties have been chosen for the fit, and the parametrization strategy has been done in the same manner as in the force field previously fitted. An acceptable final sum of squares of 15.3 has been obtained for this fit, which can reproduce the essential features of zeolites such as the structural parameters to a reasonable accuracy. A description of the calculated properties for α-quartz, the force field parameters, and some testing in selected zeolite structures can be found in the Supporting Information. This SGV force field performs remarkably well for the simulation of the dielectric and vibrational properties, better than any previous force field from those considered in this study.

The following terms and functional forms have been considered:

$$E_{zeo} = E_{Coulombic} + E_{two\text{-}body} + E_{three\text{-}body} + E_{core-shell} \quad (11)$$

$$E_{ij}^{two\text{-}body(TO)} = \frac{1}{2}k_{ij}^{r}(r_{ij} - r_0)^2 \quad (12)$$

where the Coulombic term has the same form as in eq 6, although in this case, having the atoms at zero net charge, the only (very minor) electrostatic effects come from the oxygen core and shell interactions (oxygen core and shell have the charges 4.24 and −4.24, respectively). The three-body terms for the SiOSi and OSiO interactions have the same forms as in eqs 8 and 9, respectively. The core−shell term has the same form as that in eq 10. Finally, the two-body term (eq 12) acts only between bonded Si−O atoms, as corresponds to a molecular force field.

An important consideration regarding this force field is that here the energies of rings and Si sites, which are calculated with the same equations (3 and 4, respectively), are not biased by the neglection of the electrostatic contribution, which in this case is taken into account (albeit being of zero value). Although further improvements on the definition of ring and site energies may need to include the electrostatic part, the use of this force field gives a preliminary idea on whether the electrostatics (here set to zero by definition of the molecular force field) makes a substantial contribution or it can be neglected without greatly compromising the accuracy of the results.

As for the results obtained with this SGV force field, we have repeated the calculation of the strain in rings as in Figure 3, by considering the same experimental geometries for the AST, CHA, FAU, LTA and quartz structure, but this time we substitute the parameters of the SGV force field in the energy expressions. The new results are shown in Figure 4. The absolute values for the calculated strain necessary differ between Figures 3 and 4 because the SGV force field includes a term of SiO strain which is lacking in the previous force field, and so the

new expression for the ring energy is as follows:

$$E_{\text{ring}} = \sum_{O_iSi_jO_k} E(r_{SiO}, \theta_{OSiO}) + \sum_{Si_iO_jSi_k} E(r_{SiO}, \theta_{SiOSi}) + \sum_{Si_iO_j} E(r_{SiO}) \quad (13)$$

where the sum extends over the n OSiO, n SiOSi angles, and the n SiO bonds that circumvent a ring of size n (with n Si atoms). Figure 4 shows slightly different trends than those in Figure 3 although certain aspects are retained such as the high energy of the 8- and 6MR in LTA, the intermediate energy of the 12MR in FAU, the low energy of 8MRs in quartz, and the larger energies of the 6MR than 4MRs in AST. As a tool, our ring energy analysis is of great interest to assess absolute and relative values of ring energies within a structure and across different structures, but comparison between different force fields requires careful evaluation of what terms are dominating the ring energies in each particular case. The Supporting Information also includes a reanalysis of the MEI structure with this new force field which shows again the instability of the 3MRs (1.81 kcal/mol, compared to 0.31, 0.15, 0.47, 0.64, and 0.23 for the two types of 4MRs, the 5MR, 7MR, and 12MR, respectively). Further, the new force field also reproduces the fact that the Si1 and Si4 are the most energetic sites, with the Si1 site energy (2.01 kcal/mol) being larger than that of the Si4 (1.29 kcal/mol) as it was found with the previous force field. Finally, we have also recalculated the D4R strain energies in AST, BEC, and LTA pure silica structures by using again the experimental geometries and this new SGV force field, and the new values obtained show (see Supporting Information) that 3-body D4R strains follow the same trends as the previous force field (0.84, 6.08, and 2.28 kcal/mol for AST, BEC, and LTA, respectively), but when including also the two-body (SiO) strain term, the total D4R strains are 1.16, 8.56, and 9.96 kcal/mol for AST, BEC, and LTA, respectively. This latter result shows, as well as in the previous case, that D4Rs in LTA and BEC are the most strained, whereas the D4R is much more relaxed in AST. The different result here (with respect to the previous force field) is the relative ordering between LTA and BEC (with LTA's D4R being more strained), which is due to a very large contribution of the SiO terms in the D4R strain of LTA, owing to the existing short bond distance Si−O2 = 1.568 Å (which comes from the experimental determination).

Overall, we consider that the trends shown by these two very different force fields are similar to each other and qualitatively very similar conclusions can be found in either case. The force field testing shows that the previous force field, used all through this study, shows better performance than the SGV force field for the structural characterization of pure silica zeolites, and therefore the results obtained with the former force field should be more valuable and confident.

3.6. Energy Decomposition. A pertinent theoretical consideration is the relation between the energetic magnitudes defined in this study (ring and Si-site energies) and the total potential energy of the microporous solid. The former refers to local strain while the latter has to be invoked to justify stability trends. A relation between both would justify that the overall energy of the microporous solid is controlled, at least in part, by certain local strain factors, which is the aim of this study. A relation between global and local energy has been derived as follows.

Considering the simple case of a force field of the type of eq 11, and taking into account a parametrization such as that in section 3.5 in which net charges are zero, the Coulombic term can be neglected and also the core−shell term can be considered negligible because of the short distance between oxygen core and shell. Therefore, we have the following approximation within a SGV force field:

$$E_{\text{total}} = E_{\text{two-body}} + E_{\text{three-body}} \quad (14)$$

Taking into account that the two-body is the summation of all the Si−O interactions and the three-body terms comprise the OSiO and the SiOSi angles, we have

$$E_{\text{total}} = \sum_{Si_iO_j} E(r_{SiO}) + \sum_{O_iSi_jO_k} E(r_{SiO}, \theta_{OSiO}) + \sum_{Si_iO_jSi_k} E(r_{SiO}, \theta_{SiOSi}) \quad (15)$$

Considering the energy of rings, this includes terms in SiO, OSiO, and SiOSi, but two things have to be taken into account when summing up all the rings in the structure:[55] (i) SiOSi terms are counted three times. If we consider a central Si and its four neighbors (T1−T4), rings containing, for example, the T−O−T1 term will be the rings defined by the paths T2−T−T1, T3−T−T1, and T4−T−T1; so when summing up all rings each SiOSi term is counted three times. (ii) A similar argument holds for the SiO terms, and thus they are counted three times because any SiO pair belongs to three rings.[56] Therefore, the energy of rings is as follows:

$$\sum_{\text{all rings}} E_{\text{ring}} = \sum_{O_iSi_jO_k} E(r_{SiO}, \theta_{OSiO}) + 3\sum_{Si_iO_jSi_k} E(r_{SiO}, \theta_{SiOSi}) + 3\sum_{Si_iO_j} E(r_{SiO}) \quad (16)$$

Regarding the energy of Si sites, a summation over all Si atoms of the structure gives the following expression:

$$\sum_{\text{all Si}} E_{\text{Si-site}} = \sum_{O_iSi_jO_k} E(r_{SiO}, \theta_{OSiO}) + \sum_{Si_iO_j} E(r_{SiO}) \quad (17)$$

Combining eqs 15−17 gives

$$E_{\text{total}} = \frac{1}{2}\left[\sum_{\text{all rings}} E_{\text{rings}} + \sum_{\text{all Si}} E_{\text{Si-site}}\right] - \sum_{Si_iO_j} E(r_{SiO}) - \frac{1}{2}\sum_{Si_iO_jSi_k} E(r_{SiO}, \theta_{SiOSi}) \quad (18)$$

and an equivalent and more simple expression is

$$E_{\text{total}} = \sum_{\text{all rings}} E_{\text{rings}} - 2\left[\sum_{Si_iO_jSi_k} E(r_{SiO}, \theta_{SiOSi}) + \sum_{Si_iO_j} E(r_{SiO})\right] \quad (19)$$

Equation 19 shows that, within this SGV force field, the total energy of the solid can be expressed in terms of the ring energies plus a subtracted term containing the SiOSi and SiO interactions. A complete decomposition of the total energy in terms of energies of rings and Si sites is not possible, but calculations performed with the SGV force field (the parameters are available in the Supporting Information) on the optimized zeolite structures—not shown for the sake of brevity—clearly indicate that the SiO term amounts to less than 1% of the total energy, and therefore the following approximation can be made:

$$E_{\text{total}} \cong \sum_{\text{all rings}} E_{\text{rings}} - 2\sum_{Si_iO_jSi_k} E(r_{SiO}, \theta_{SiOSi}) \quad (20)$$

Equation 20, within the SGV force field, is interesting because it relates the total energy with the ring strain minus a term containing twice the SiOSi energy. Equation 20 is equivalent to the following:

$$E_{\text{total}} \cong \sum_{O_iSi_jO_k} E(r_{SiO}, \theta_{OSiO}) + \sum_{Si_iO_jSi_k} E(r_{SiO}, \theta_{SiOSi}) = \text{Strain(OSiO)} + \text{Strain(SiOSi)} \quad (21)$$

where the terms in OSiO and SiOSi are considered as strains because the zero energy, within the SGV force field, is taken as a structure with tetrahedral OSiO angles and with angles SiOSi equal to 145°. Equation 21, as stated in the Introduction and throughout this work, points to the idea of taking into account that the strain has several sources, and although traditionally SiOSi has been the major one intuitively considered, OSiO may also play an important role in many cases. A proper and automated computation of strains has been developed here, and this allows a separation of the effects of strain and a quantification of the weights of each contribution.

4. Conclusions

Adequate counting of rings through the vertex symbols allows the characterization of all the rings present in a zeolite structure. This feature is exploited by a computer program which characterizes all the rings present in any zeolite structure. Classification of SiOSi and OSiO angles with respect to the ring they belong to allows one to find whether relations between the ring size and the angle value exist. Further, with the angle values, an estimation of the corresponding associated strain is performed, and this allows one to find the strain of each ring as well as the components of the strain. This allows an identification of sources of local instability within the zeolite topology. An appropriate energy functional for the three-body (OSiO and SiOSi) terms has been chosen, and a new atomistic force field, starting from a previous force field by Vessal et al.,[30] has been parametrized. Previous approaches used to relate energetic stability with global properties such as framework density of the zeolite and our present study allows characterization of the strain and relaxation of local parts of the structure. This can be used to explain trends which were not fully accounted for when only global properties were invoked. Also, mechanisms of preferential substitution of heteroatoms in certain T sites can be investigated within this approach. A refinement on the energy functional and parameters can be a subject of further studies aimed to calculate more accurately the energy of the system and the different terms, in particular regarding the role of the electrostatic contribution. Finally, only SiO_2 zeolite structures are treated here simply and clearly as a first case study of this methodology, but this approach could also be extended in the future to study aluminosilicate and germanosilicate zeotypes, among others.

Acknowledgment. We thank Centro de Proceso de Datos of the Universidad Politecnica de Valencia for the use of their computational facilities. We thank the Spanish Government for funding through Project MAT2003-07769-C02-01. We thank an anonymous referee for suggestions on the energy decomposition.

Supporting Information Available: Properties of quartz with SGV force field, SGV parameters, cell parameters of zeolites optimized with the SGV force field, energies of MEI zeolite with the SGV force field, strain energies of double four rings with the SGV force field. This material is available free of charge via the Internet at http://pubs.acs.org.

References and Notes

(1) Corma, A. *J. Catal.* **2003**, *216* (1−2), 298.
(2) Davis, M. E. *Science* **2004**, *305*, 480.
(3) (a) Burton, A.; Elomari, S.; Chen, C. Y.; Medrud, R. C.; Chan, I. Y.; Bull, L. M.; Kibby, C.; Harris, T. V.; Zones, S. I.; Vittoratos, E. S. *Chem.−Eur. J.* **2003**, *9* (23), 5737. (b) Burton, A.; Elomari, S. *Chem. Commun.* **2004**, *22*, 2618. (c) Zanardi, S.; Alberti, A.; Cruciani, G.; Corma, A.; Fornes, V.; Brunelli, M. *Angew. Chem., Int. Ed.* **2004**, *43*, 4933. (d) Harbuzaru, B.; Paillaud, J.-L.; Patarin, J.; Bats, N. *Science* **2004**, *304*, 990. (e) Strohmaier, K. G.; Vaughan, D. E. W. *J. Am. Chem. Soc.* **2003**, *125* (51), 16035. (f) Corma, A.; Diaz-Cabañas, M. J.; Rey, F.; Nicolopoulos, S.; Boulahya, K. *Chem. Commun.* **2004**, 1356. (g) Morris, R. E.; Burton, A.; Bull, L. M.; Zones, S. I. *Chem. Mater.* **2004**, *16*, 2844−2851. (h) Josien, L.; Simon Masseron, A.; Gramlich, V.; Patarin, J.; Rouleau, L. *Chem.−Eur. J.* **2003**, *9*, 856−861.
(4) Corma, A.; Davis, M. E. *Chem. Phys. Chem.* **2004**, *5* (3), 304.
(5) O'Keeffe, M.; Hyde, S. T. *Zeolites* **1997**, *19*, 370. Vertex symbols are defined as the size (and multiplicity) of the shortest circuit contained in each angle of a vertex (in zeolites, vertex are tetrahedral atoms), the latter angle in zeolites and tectosilicates being defined by chemically bonded OSiO links.
(6) Galeener, F. L. *Solid State Commun.* **1982**, *44* (7), 1037.
(7) NMR distributions in vitreous silica as well as in silica crystals indicate that the OSiO angle distributions peak very narrowly at the equilibrium value. See Kuzuu, N.; Yoshie, H.; Tamai, Y.; Wang, C. *J. Non-Cryst. Solids* **2004**, *349*, 319 and references therein.
(8) Garces, J. M. *Adv. Mater.* **1996**, *8* (5), 434.
(9) (a) Piccione, P. M.; Camblor, M. A.; Navrotsky, A.; Davis, M. E. *J. Phys. Chem. B* **2000**, *104*, 10001. (b) Piccione, P. M.; Yang, S.; Navrotsky, A.; Davis, M. E. *J. Phys. Chem. B* **2002**, *106*, 3629.
(10) Brunner, G. O. *Zeolites* **1993**, *13*, 88.
(11) Petrovic, I.; Navrotsky, A.; Davis, M. E.; Zones, S. I. *Chem. Mater.* **1993**, *5*, 1805.
(12) Akporiaye, D. E.; Price, G. D. *Zeolites* **1989**, *9*, 32.
(13) Henson, N. J.; Gale, J. D.; Cheetham, A. K. *Chem. Mater.* **1994**, *6*, 1647.
(14) (a) Hyde, S. T.; Ninham, B. W.; Blum, Z. *Acta Crystallogr., Sect. A: Found. Crystallogr.* **1993**, *49*, 586.
(15) (a) Zwijnenburg, M. A.; Bromley, S. T.; Jansen, J. C.; Maschmeyer, T. *Chem. Mater.* **2004**, *16*, 12. (b) Zwijnenburg, M. A.; Bromley, S. T.; Foster, M. D.; Bell, R. G.; Delgado-Friedrichs, O.; Jansen, J. C.; Maschmeyer, T. *Chem. Mater.* **2004**, *16*, 3809.
(16) Gibbs, G. V.; Meagher, E. P.; Newton, M. D.; Swanson, D. K. In *Structure and Bonding in Crystals*; O'Keeffe, M., Navrotsky, A., Eds.; Academic Press: New York, 1981; Vol. 1, p 195.
(17) Hammonds, K. D.; Heine, V.; Dove, M. T. *J. Phys. Chem. B* **1998**, *102*, 1759.
(18) Newton, M. D. *Structure and Bonding in Crystals*; O'Keeffe, M., Navrotsky, A., Eds.; Academic Press: New York, 1981; Vol. 1, p 175.
(19) Newton, M. D.; Gibbs, G. V. *Phys. Chem. Miner.* **1980**, *6*, 221.
(20) Baerlocher, C.; Meier, W. M.; Olson, D. H. *Atlas of Zeolite Structure Types*, 5th ed.; Elsevier: Amsterdam, The Netherlands, 2001; http://www.iza-online.org.
(21) Gale, J. D.; Sastre, G. *Microporous Mesoporous Mater.* **2001**, *43*, 27.
(22) (a) Jackson, R. A.; Catlow, C. R. A. *Mol. Simul.* **1988**, *1*, 207. (b) *Computer Simulation of Solids*; Catlow, C. R. A., Mackrodt, W. C., Eds.; Lecture Notes in Physics, Vol. 166; Springer: Berlin, 1982. (c) Gale, J. D. *J. Chem. Soc., Faraday Trans.* **1997**, *93*, 629. (d) Gale, J. D. *J. Phys. Chem. B* **1998**, *102*, 5423.
(23) Sanders, M. J.; Leslie, M.; Catlow, C. R. A. *J. Chem., Soc. Chem. Commun.* **1984**, 1271.
(24) Blake, N. P.; Weakliem, P. C.; Metiu, H. *J. Phys. Chem. B* **1998**, *102*, 67.
(25) Sefcik, T.; Deniralp, G.; Cagin, T.; Goddard, W. A., III. *J. Comput. Chem.* **2002**, *23*, 1507.
(26) Huang, L.; Kieffer, J. *J. Chem. Phys.* **2003**, *118*, 1487.
(27) Nasluzov, V. A.; Ivanova, E. A.; Shor, A. M.; Vayssilov, G. N.; Birkenheuer, U.; Rösch, N. *J. Phys. Chem. B* **2003**, *107*, 2228.
(28) Vink, R. L. C.; Barkema, G. T. *Phys. Rev. B: Condens. Matter Mater Phys.* **2003**, *67* (24), Article 245201.
(29) Vashishta, P.; Kalia, R. K.; Rino, J. P.; Ebbsjö, I. *Phys. Rev. B: Condens. Matter Mater. Phys.* **1990**, *41*, 12197.
(30) Vessal, B.; Leslie, M.; Catlow, C. R. A. *Mol. Simul.* **1989**, *3*, 123.
(31) Engelhardt, G.; Nofz, M.; Forkel, K.; Wihsmann, I. G.; Magi, M.; Samosen, A.; Lippmaa, E. *Phys. Chem. Glasses* **1985**, *26*, 157.
(32) Gale, J. D. *Philos. Mag. B* **1996**, *73*, 3.
(33) (a) Gale, J. D. *J. Chem. Soc., Faraday Trans.* **1997**, *93*, 629. (b) Gale, J. D.; Rohl, A. L. *Mol. Simul.* **2003**, *29* (5), 291.

(34) The zeoTsites software can be obtained by request to gsastre@itq.upv.es.

(35) Lawton, S. L.; Rohrbaugh, W. J. *Science* **1990**, *247*, 1319.

(36) Zeolite topologies are named by a three letter code assigned by the International Zeolite Association-Structure Commission listed in ref 20.

(37) (a) Brunner, G. O. *J. Solid State Chem.* **1979**, *29*, 41. (b) Chakoumakos, B. C.; Hill, R. J.; Gibbs, G. V. *Am. Mineral.* **1981**, *66*, 1237. (c) Tossell, J. A.; Gibbs, G. V. *Acta Crystallogr., Sect. A: Found Crystallogr.* **1978**, *34*, 463. (d) Meier, W. M. *Pure Appl. Chem.* **1986**, *58*, 1323.

(38) Sabater, M. J.; Sastre, G. *Chem. Mater.* **2001**, *13*, 4520.

(39) Lawton, S. L.; Ciric, J.; Kokotailo, G.; Griffin, G. W. *Acta Crystallogr. Sect. C: Cryst. Struct. Commun.* **1985**, *C41*, 1683.

(40) Gale, J. D.; Cheetham, A. K. *Zeolites* **1992**, *12*, 674.

(41) Hriljac, J. J.; Eddy, M. M.; Cheetham, A. K.; Donohue, J. A.; Ray, G. J. *J. Solid State Chem.* **1993**, *106*, 66−72.

(42) Flanigen, E. M.; Patton, R. L. U.S. Patent 4073865, 1978.

(43) For the topologies referred see the Atlas of Zeolite Structure Types (ref 20). And for the materials the references are as follows: (a) (ITQ-21) Corma, A.; Diaz-Cabañas, M. J.; Martinez-Triguero, J.; Rey, F.; Rius, J. *Nature* **2002**, *418*, 514. (b) (ITQ-32) Cantin, A.; Corma, A.; Leiva, S.; Rey, F.; Rius, J.; Valencia, S. *J. Am. Chem. Soc.* **2005**, *127* (33), 11560. (c) (ITQ-29) Corma, A.; Rey, F.; Rius, J.; Sabater, M. J.; Valencia, S. *Nature* **2004**, *431*, 287.

(44) (a) Kessler, H.; Patarin, J.; Schott-Darie, C. *Stud. Surf. Sci. Catal.* **1994**, *85*, 75. (b) Guth, J. L.; Kessler, H.; Wey, R. In *New Developments in Zeolite Science and Technology*; Murakami, Y., Ijima, A., Ward, J. W., Eds.; Elsevier: Amsterdam, The Netherlands, 1986; p 121. (c) Camblor, M. A.; Villaescusa, L. A.; Diaz-Cabañas, M. J. *Top. Catal.* **1999**, *9*, 59.

(45) O'Keeffe, M.; Yaghi, O. M. *Eur. J. Chem.* **1999**, *5* (10), 2796.

(46) (a) Li, Q.; Navrotsky, A.; Rey, F.; Corma, A. *Microporous Mesoporous Mater.* **2003**, *59*, 177. (b) Li, Q.; Navrotsky, A.; Rey, F.; Corma, A. *Microporous Mesoporous Mater.* **2004**, *74*, 87.

(47) Smirnov, K. S.; Bougeard, D. *J. Raman Spectrosc.* **1993**, *24*, 255.

(48) Barrett, P. A.; Camblor, M. A.; Corma, A.; Jones, R. H.; Villaescusa, L. A. *Chem. Mater.* **1997**, *9*, 1713.

(49) Camblor, M. A.; Corma, A.; Diaz-Cabañas, M. J.; Baerlocher, C. *J. Phys. Chem. B* **1998**, *102*, 44.

(50) Lobo, R. F.; Pan, M.; Chan, I.; Li, H. X.; Medrud, R. C.; Zones, S. I.; Crozier, P. A.; Davis, M. E. *Science* **1993**, *262*, 1543.

(51) Villaescusa, L. A.; Barrett, P. A.; Camblor, M. A. *Chem. Mater.* **1998**, *10*, 3966.

(52) Newsam, J. M.; Treacy, M. M. J.; Koetsier, W. J.; de Gruyter, C. B. *Proc. R. Soc. London, Ser. A* **1988**, *420*, 375.

(53) Liu, Z.; Ohsuna, T.; Terasaki, O.; Camblor, M. A.; Diaz-Cabañas, M. J.; Hiraga, K. *J. Am. Chem. Soc.* **2001**, *123*, 5370.

(54) Diaz-Cabañas, M. J.; Barrett, P. A.; Camblor, M. A. *Chem. Commun.* **1998**, 1881.

(55) This ring counting does not include rings corresponding to the subindex of the vertex symbol.

(56) Naming the four oxygens attached to a Si as 1, 2, 3, 4 gives six rings attached to a Si defined by the paths of the O−Si−O links which are: 12, 13, 14, 23, 24, 34. Any oxygen (1, 2, 3, 4) appears in three rings and that is why any SiO link is counted three times when counting the rings of the structure.